nature communications

Article

https://doi.org/10.1038/s41467-024-52193-w

EXTL3 and NPC1 are mammalian host factors for *Autographa californica* multiple nucleopolyhedrovirus infection

Received: 25 January 2024

Accepted: 28 August 2024

Published online: 04 September 2024

Check for updates

Yuege Huang[1,8], Hong Mei[2,8] ✉, Chunchen Deng[2,3], Wei Wang[2], Chao Yuan[2,3], Yan Nie[2], Jia-Da Li[1,4] ✉ & Jia Liu[2,3,5,6,7] ✉

Baculovirus is an obligate parasitic virus of the phylum *Arthropoda*. Baculovirus including *Autographa californica* multiple nucleopolyhedrovirus (AcMNPV) has been widely used in the laboratory and industrial preparation of proteins or protein complexes. Due to its large packaging capacity and non-replicative and non-integrative natures in mammals, baculovirus has been proposed as a gene therapy vector for transgene delivery. However, the mechanism of baculovirus transduction in mammalian cells has not been fully illustrated. Here, we employed a cell surface protein-focused CRISPR screen to identify host dependency factors for baculovirus transduction in mammalian cells. The screening experiment uncovered a series of baculovirus host factors in human cells, including exostosin-like glycosyltransferase 3 (EXTL3) and NPC intracellular cholesterol transporter 1 (NPC1). Further investigation illustrated that EXTL3 affected baculovirus attachment and entry by participating in heparan sulfate biosynthesis. In addition, NPC1 promoted baculovirus transduction by mediating membrane fusion and endosomal escape. Moreover, in vivo, baculovirus transduction in *Npc1*$^{-/+}$ mice showed that disruption of *Npc1* gene significantly reduced baculovirus transduction in mouse liver. In summary, our study revealed the functions of EXTL3 and NPC1 in baculovirus attachment, entry, and endosomal escape in mammalian cells, which is useful for understanding baculovirus transduction in human cells.

Baculoviruses are enveloped, double-strand DNA viruses comprising large genomes ranging from 80 to 180 kilobase pairs[1]. As the first baculovirus with full sequence information, AcMNPV has a genome of 133,894 nucleotides in size that contains 154 predicted non-overlapping open reading frames[2]. In nature, AcMNPV produces two structurally and functionally distinct virion forms, budded virions (BVs) and occlusion-derived virions (ODVs)[3]. BVs occur primarily in a loose viral envelope containing a single nucleocapsid, while ODVs have more than one nucleocapsid in a single envelope[4]. Although the two virion forms may share some common nucleocapsid proteins such as P39, the envelope components are largely different. BVs have envelope glycoproteins GP64, whereas ODVs contain polyhedral envelope protein P32-34, polyhedrin P29[4,5], and per os infectivity factors (PIFs) that are required for the infection in insect gut[6,7]. BVs capture cell

[1]Furong Laboratory, Center for Medical Genetics, School of Life Sciences, Central South University, Changsha, Hunan, China. [2]Shanghai Institute for Advanced Immunochemical Studies, ShanghaiTech University, Shanghai, China. [3]School of Life Science and Technology, ShanghaiTech University, Shanghai, China. [4]Hunan Key Laboratory of Animal Models for Human Diseases, Changsha, Hunan, China. [5]Shanghai Clinical Research and Trial Center, Shanghai, China. [6]Guangzhou Laboratory, Guangzhou International Bio Island, Guangzhou, Guangdong, China. [7]Shanghai Asiflyerbio Biotechnology, Shanghai, China. [8]These authors contributed equally: Yuege Huang, Hong Mei. ✉e-mail: meihong@shanghaitech.edu.cn; lijiada@sklmg.edu.cn; liujia@shanghaitech.edu.cn

membranes as their envelopes and transmit within the hosts. By contrast, ODVs acquire envelopes from cell nuclear membrane and transmit between hosts[8,9]. BVs enter cells through receptor-mediated endocytosis[10,11], while ODVs appear to fuse directly with the plasma membrane[12,13].

Like other enveloped viruses, the interactions between envelope glycoproteins and host cell receptors are important for baculovirus entry. GP64 and F protein are the major envelope glycoproteins of *lepidopteran* nucleopolyhedrovirus (NPVs)[14]. In group I NPVs such as AcMNPV, GP64 functions as a fusion protein mediating viral entry into host cells[10], while the F protein Ac23 seemed dispensable for infection in insect cells[14,15]. Different from group I NPVs, group II NPVs such as *Spodoptera exigua* MNPV and *Lymantria dispar* MNPV do not have GP64 protein and utilize F protein as the fusion protein for virus entry[16–18].

As a class III fusion protein, AcMNPV GP64 protein has 512 amino acids[19,20] constituting five domains or structurally distinct regions, among which domain I contains fusion peptide and receptor binding peptide[10,19]. Different from class I and class II fusion proteins, GP64 does not undergo proteolytic cleavage[20,21]. The membrane fusion process of AcMNPV is triggered by a reversible, pH-dependent conformational change of GP64[22], which remains trimeric in pre-fusion and post-fusion states[19]. Despite the existing studies in insect cells, the cellular receptor for GP64 binding in mammalian cells has not been reported.

AcMNPV is one of the most widely used baculoviruses in laboratory research and industry[23]. Baculovirus expression vector system (BEVS) was developed in the 1980s by using BVs as a transgene delivery vector to insect cells[24]. BEVS has now become one of the most widely used expression systems in the laboratory and industry for production of recombinant proteins[25], virus-like particles[26,27], and baculovirus-based vaccines[28–33].

In addition to gene transfer into insect cells, baculovirus has been employed as gene delivery vectors in mammalian cells[34–36]. Baculovirus is capable of delivering a variety of genome editing tools into human cells, including zinc finger nucleases (ZFNs)[37–39], TALENs[40], CRISPR-Cas[41], and CRISPR-based prime editors[42]. Genome editing in primary neurons and induced pluripotent stem cells (iPSCs) has also been achieved by baculovirus delivery of CRISPR-Cas9. Compared to other viral vectors[43,44], the non-replicative and non-integrative natures render baculovirus a potentially safe gene therapy vector. Another notable advantage of baculovirus as a gene transfer vector lies in its large packaging capacity, which enables the delivery of large genome-editing tools such as prime editors in a single virion[42].

More importantly, baculovirus has been exploited for in vivo gene delivery in mammals. Direct injection of baculovirus in mouse and rat brains could efficiently transduce neural cells[45]. Intravitreal baculovirus injection mediated gene transfer in mouse and rabbit eyes[46,47]. In cancer mouse models, intratumoral baculovirus injection was shown to be capable of delivering antiangiogenic proteins for cancer therapy[48,49]. Engineering efforts have shown that the transduction efficiency of baculovirus in mammalian cells in vitro and in vivo could be enhanced[50–53].

Despite the widespread applications, the mechanism of baculovirus transduction in mammalian cells is yet poorly understood. Previous studies have shown that polybrene and heparin can inhibit baculovirus transduction in mammalian cells, suggesting an important role of electrostatic interactions[54,55]. Syndecan-1 (SDC-1) was also found to be important for baculovirus binding on mammalian cells[56]. Other studies suggested that baculovirus attachment on mammalian cells depended on cell surface phospholipids[57] and cholesterol[58,59]. Meanwhile, restriction factors that limit baculovirus transduction in mammalian cells have also been identified[60]. Nevertheless, there is yet no systematic investigation on baculovirus host factors in mammalian cells.

Genetic screen using clustered regularly interspaced short palindromic repeats (CRISPR) has been widely used in the dissection of host-pathogen interactions[61]. In a previous study, we established a cell surface protein-focused CRISPR library, so-called surfaceome CRISPR (SfCRISPR), and showed that this library could efficiently identify rhinovirus host factors[62]. In the present study, we employed this sfCRISPR library to perform forward genetic screen on a recombinant baculovirus carrying *EGFP* transgene (Bac-EGFP). Two rounds of negative selection identified several candidate host dependency factors for baculovirus transduction in human cells, including exostosin-like glycosyltransferase 3 (EXTL3) and Niemann-Pick C1 (NPC1). In-depth analyses illustrated the role of EXTL3 and NPC1 for the in vitro and in vivo baculovirus transduction in mammalian cells.

Results

Identification of baculovirus host factors in HEK-293T cells using SfCRISPR screen

To identify cell surface host factors of baculovirus in mammalian cells, we performed genetic screen using a previously described cell surfaceome CRISPR library (SfCRISPR) that contained sgRNAs targeting to 1344 cell surface protein-coding genes in human genome[62]. We examined several cell lines for baculovirus transduction and found that HEK-293T cells exhibited highest transduction rate (Supplementary Fig. 1a), which was important for reducing the background in the negative EGFP selection (Fig. 1a). HEK-293T cells were transduced with lentivirus (LV) carrying the SfCRISPR library. Next-generation sequencing (NGS) analysis showed that this cell library had full coverage of sgRNAs (Supplementary Fig. 1b) with a uniform distribution as predicted (Supplementary Fig. 1c). In addition, we analyzed the shift of sgRNAs targeting essential and nonessential genes by comparing the sgRNAs at 5 days and 12 days after LV transduction and found that sgRNAs targeting essential genes were significantly depleted (Supplementary Fig. 1d) as described[63]. These results suggested that the library was constructed successfully and was qualified for downstream phenotypic screen.

The validated cell library containing cell surface protein knockouts was then infected with baculovirus harboring enhanced green fluorescent protein transgene (Bac-EGFP). The Bac-EGFP-transduced cells were sorted by flow cytometry for enriching EGFP negative cells (Fig. 1a). This negative selection approach allowed enrichment of cells deficient in baculovirus host factors. Two rounds of negative selection were performed and sgRNA enrichment was observed (Supplementary Fig. 1e). With the process of negative selection, we observed an increased frequency of EGFP negative cells in round 2 selection, suggesting of successfully imposed selection pressure (Supplementary Fig. 2a, b).

The cells after round 1 and round 2 selection were collected and the genomic DNA was extracted and analyzed by NGS. The genes with enriched sgRNAs were determined using modified robust rank aggregation (a-RRA) analyses in the MAGeCK pipeline (MAGeCK score) and candidate gene hits with an FDR cutoff of 0.05 were displayed (Fig. 1b, c and Supplementary Data File 1). Seven candidate hits were consistently enriched in both rounds of selection, including exostosin-like glycosyltransferase 3 (EXTL3), Niemann-Pick C1 (NPC1), SREBP cleavage activating protein (SCAP), FAM20B glycosaminoglycan xylosylkinase (FAM20B), membrane-bound transcription factor site-2 protease (MBTPS2), glucuronic acid epimerase (GLCE) and transmembrane 9 superfamily member 3 (TM9SF3). For each candidate gene, two sgRNAs were designed to construct knockout cells in HEK-293T cells (Supplementary Fig. 3a–g).

It was found that the knockout of *EXTL3*, *NPC1*, *SCAP*, *MBTPS2* and *GCLE* with both sgRNAs significantly reduced Bac-EGFP transduction (Fig. 1d). Importantly, *EXTL3* and *NPC1* knockout reduced EGFP-positive cells to less than 50% of that in the non-targeting sgRNA group (Fig. 1d). Thus, subsequent experiments were focused on studying the

https://doi.org/10.1038/s41467-024-52193-w

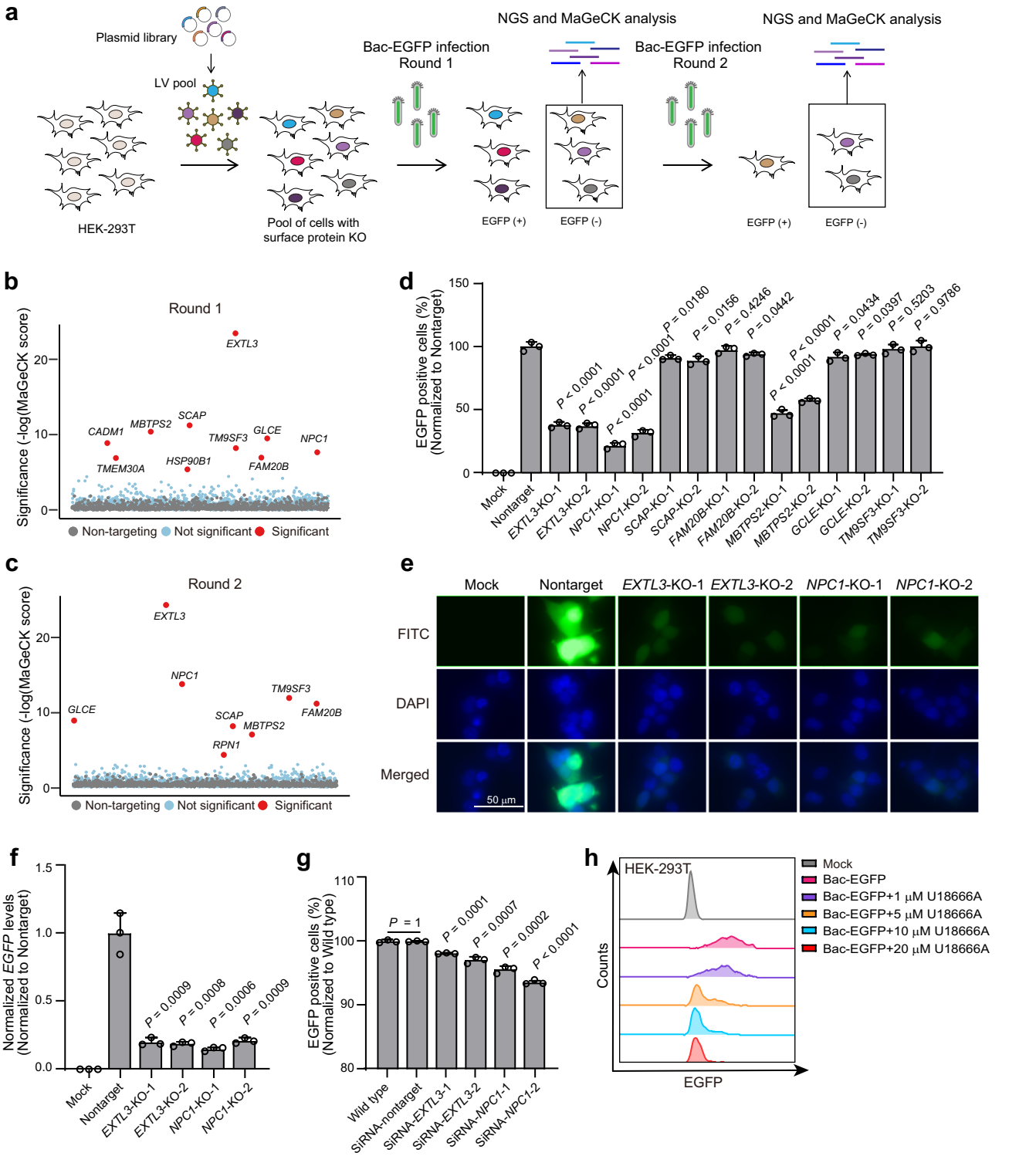

Fig. 1 | Identification of NPC1 and EXTL3 as baculovirus host factors in HEK-293T. a Flowchart showing the negative selection approach for baculovirus host factor identification using surfaceome CRISPR screen. Candidate gene hits identified from the first (**b**) and second (**c**) rounds of selection. **d** The effects of knockout of the seven candidate genes on Bac-EGFP transduction, as determined by flow cytometry analyses. The *p*-value between Nontarget and *EXTL3*-KO-1, *EXTL3*-KO-2, *NPC1*-KO-1, *NPC1*-KO-2, *MBTPS2*-KO-1 and *MBTPS2*-KO-2 groups are 1e-5, 1e-5, 6e-6, 1e-5, 4e-5 and 4e-5, respectively. **e** Fluorescence imaging of Bac-EGFP infected cells. The experiment is repeated three times independently with similar results. **f** RT-qPCR quantification of *EGFP* mRNA in the lysate of *EXTL3* and *NPC1* knockout cells at 48 h post-Bac-EGFP transduction. β-actin is used as an internal control. **g** Evaluation of the effects of *EXTL3* and *NPC1* knockdown on Bac-EGFP transduction. The *p*-value between SiRNA-nontarget and SiRNA-*NPC1*-2 groups is 1e-5. **h** Evaluation of the effects of NPC1 inhibitor U18666A on Bac-EGFP transduction. For (**d**, **f**, and **g**), Data are presented as mean ± SD ($n = 3$) from three biological replicates. The significant difference is analyzed by two-tailed unpaired Student's *t*-test. Mock group is the PBS treatment without baculovirus. Source data are provided as a Source Data file.

https://doi.org/10.1038/s41467-024-52193-w

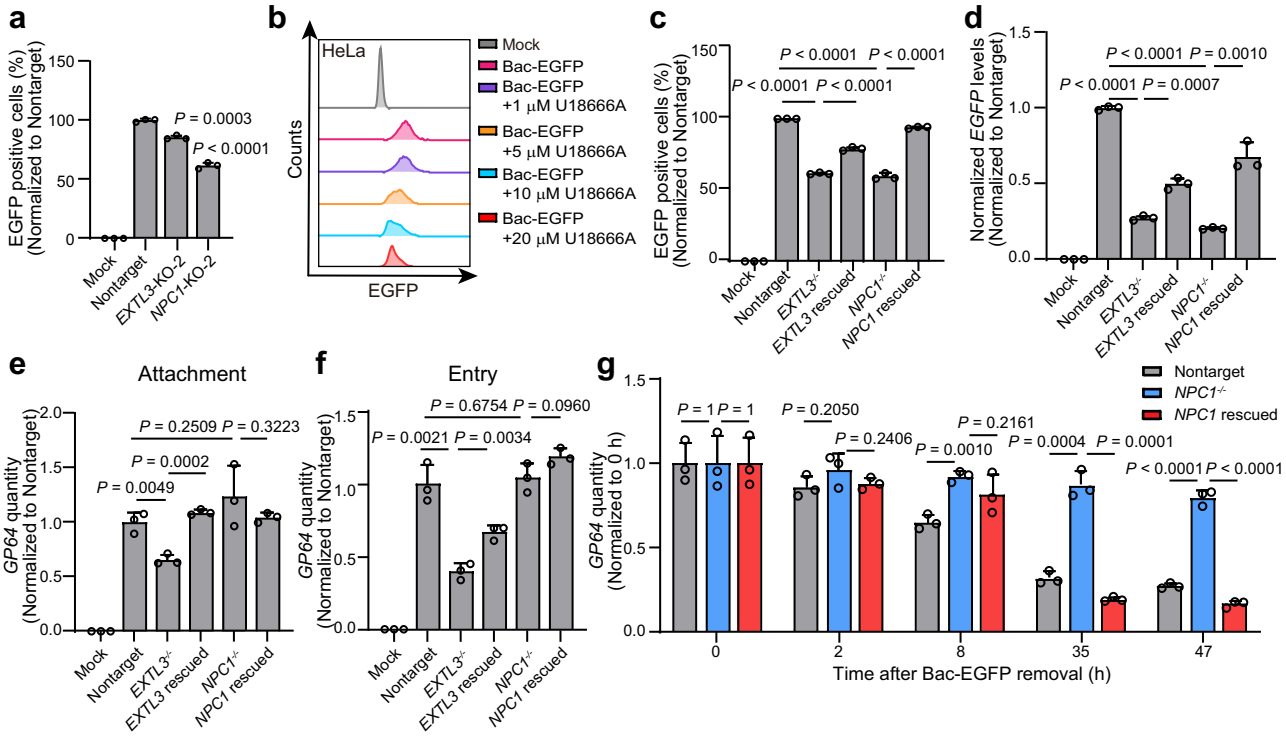

Fig. 2 | Determination of the functions of EXTL3 and NPC1 in HeLa cells. **a** Evaluation of the effects of *EXTL3* and *NPC1* knockouts on Bac-EGFP transduction, as determined by flow cytometry analyses. The *p*-value between Nontarget and *NPC1*-KO-2 groups is 2e-5. **b** Evaluation of the effects of NPC1 inhibitor U18666A on Bac-EGFP transduction. Evaluation of the effects of *EXTL3* and *NPC1* knockouts and overexpression rescue on Bac-EGFP transduction, as determined by flow cytometry (EGFP protein) (**c**) and RT-qPCR (*EGFP* mRNA) (**d**). β-actin is used as an internal control for RT-qPCR. For (**c**), the *p*-values between Nontarget and *EXTL3*$^{-/-}$ and *NPC1*$^{-/-}$ groups are 5e-8 and 5e-6, respectively. The *p*-value between *EXTL3*$^{-/-}$ and *EXTL3* rescued groups is 2e-5. The *p*-value between *NPC1*$^{-/-}$ and *NPC1* rescued groups is 1e-5. For (**d**), the *p*-value between Nontarget and *EXTL3*$^{-/-}$ and *NPC1*$^{-/-}$ groups are 4e-7 and 7e-8, respectively. Evaluation of the effects of *EXTL3* or *NPC1* knockout and overexpression rescue on Bac-EGFP attachment (**e**) and entry (**f**). **g** qPCR quantification of the intracellular baculovirus genome *GP64* gene after Bac-EGFP transduction in non-targeting sgRNA, *NPC1*$^{-/-}$ and *NPC1* rescued HeLa cells. Bac-EGFP is incubated with cells at an MOI of 2 for 1 h and then removed from the medium. The total *GP64* in each well is quantified. The *p*-values between *NPC1*$^{-/-}$ and Nontarget and *NPC1* rescued group at 47 h are 5e-5 and 3e-5, respectively. For (**a**), (**c**–**g**), Data are presented as mean ± SD ($n = 3$) from three biological replicates. The significant difference is analyzed by two-tailed unpaired Student's *t*-test. Mock group is the PBS treatment without baculovirus. Source data are provided as a Source Data file.

function of EXTL3 and NPC1. EXTL3 contains a glycosyltransferase domain and plays a critical role in the biosynthesis of heparan sulfate, which can facilitate viral attachment and entry[64–66]. NPC1 is a known host factor for various clinically important viruses[67,68]. Therefore, in the subsequent experiments, we focused our investigation on the functions and mechanisms of EXTL3 and NPC1 in baculovirus transduction.

Validation of EXTL3 and NPC1 as host dependency factors of baculovirus

In consistency with the flow cytometry experiments, fluorescent microscopy imaging showed that *EXTL3* or *NPC1* knockout reduced Bac-EGFP transduction (Fig. 1e). Moreover, RT-qPCR analysis revealed decreased mRNA expression of *EGFP* transgene in *EXTL3* and *NPC1* knockout cells (Fig. 1f). Similar to Bac-EGFP transduction, baculovirus carrying tdTomato (Bac-tdTomato) also exhibited reduced transduction efficiency in *EXTL3* and *NPC1* knockout HEK-293T cells (Supplementary Fig. 4a, b). In addition, we designed *EXTL3*- and *NPC1*-targeting siRNAs (Supplementary Fig. 4c, d) and found that knockdown of *EXTL3* and *NPC1* could also suppress baculovirus transduction albeit with lesser impact than *EXTL3* and *NPC1* knockout (Fig. 1g). The function of NPC1 in baculovirus transduction was further validated by U18666A, a small molecule inhibitor of NPC1. It was found that U18666A inhibited Bac-EGFP transduction in a dose-dependent manner in HEK-293T cells (Fig. 1h). Collectively, these results demonstrated that EXTL3 and NPC1 were host dependency factors for baculovirus transduction in human cells.

Evaluation of the functions of EXTL3 and NPC1 in baculovirus attachment, entry, and endosomal escape

Similar to the results in HEK-293T cells, *EXTL3* and *NPC1* knockout in HeLa cells (Supplementary Fig. 5a) inhibited Bac-EGFP transduction (Fig. 2a and Supplementary Fig. 5b). The NPC1 inhibitor U18666A reduced EGFP fluorescence in Bac-EGFP-transduced HeLa cells (Fig. 2b and Supplementary Fig. 5c). Next we constructed single clones of HeLa cells for *EXTL3* and *NPC1* knockouts respectively. These single clones were confirmed to contain genomic modifications at both alleles of *EXTL3* and *NPC1* (Supplementary Fig. 5d). Consistent with the above results, *EXTL3*$^{-/-}$ and *NPC1*$^{-/-}$ clones exhibited reduced Bac-EGFP transduction, as determined by EGFP expression at both protein (Fig. 2c and Supplementary Fig. 5e) and mRNA (Fig. 2d) levels. Moreover, rescue experiments by overexpressing *EXTL3* and *NPC1* in corresponding knockout single clones (Supplementary Fig. 5f, g) restored baculovirus transduction (Fig. 2c, d and Supplementary Fig. 5h).

To determine the roles of EXTL3 and NPC1 during baculovirus transduction, we investigated their functions in viral attachment and entry. For viral attachment assay, Bac-EGFP was incubated with cells at 4 °C for 1 h. The cells with attached baculovirus were harvested and lysed for qPCR quantification of viral loads. For virus entry assay, Bac-EGFP was incubated with cells first at 4 °C for 1 h and then at 37 °C for 45 min to initiate the internalization of Bac-EGFP. Surface-bound Bac-EGFP was removed by trypsin treatment and the internalized virus was quantified by qPCR. It was found that *EXTL3*$^{-/-}$ cells significantly reduced baculovirus attachment and entry, which could be restored by

EXTL3 overexpression (Fig. 2e, f). By contrast, *NPC1* knockout or overexpression rescue did not significantly affect baculovirus attachment or entry (Fig. 2e, f). Taken together, these results suggested that EXTL3, but not NPC1, was involved in baculovirus attachment and entry.

To explore whether NPC1 participated in any transduction process following attachment and entry, we sought to analyze the function of NPC1 on endosomal escape. It is known that baculovirus does not replicate in mammalian cells[69], thus we monitored the decay rate of intracellular baculovirus genome in an approach similar to a previous study[62]. Non-targeting sgRNA-treated, *NPC1*$^{-/-}$ and *NPC1* rescued HeLa cells were transduced with Bac-EGFP for 1 h and then the virus-containing medium was replaced with fresh medium. The total *GP64* quantity in each well was monitored over a course of 47 h after the removal of virus. It was found that baculovirus DNA decreased in a time-dependent manner (Fig. 2g), suggesting that the cellular DNA degradation machinery was active toward baculovirus genome. Importantly, *NPC1*$^{-/-}$ cells retained significantly higher level of baculovirus genome than non-targeting sgRNA-treated cells starting from 8 h after removal of virus (Fig. 2g). Consistently, *NPC1* overexpression rescue significantly reduced baculoviral genome quantity at 35 h and 47 h in comparison to *NPC1*$^{-/-}$ cells. To exclude the possibility that the difference in intracellular viral genome was due to differential cell proliferation, we examined the proliferation of non-targeting sgRNA, *NPC1*$^{-/-}$ and *NPC1* rescued cells and observed minor difference between each group (Supplementary Fig. 5i). These data showed that knockout of *NPC1* could extend the persistence of intracellular baculovirus genome and thus indicated a potential role of NPC1 in baculovirus endosomal escape.

The above results prompted us to expand the investigation on the mechanism of retention of Bac genome. Bafilomycin A1 (BafA1) is a specific inhibitor of V-type ATPases[70] and has been reported to be capable of inhibiting endosomal escape of viruses by suppressing endosomal acidification[71,72]. In the present study, it was found that pretreatment of cells with BafA1 could prolong the retention of intracellular Bac genome (Supplementary Fig. 6a), similar to the effects of *NPC1* knockout. In addition, BafA1 treatment had minor impact on cell proliferation (Supplementary Fig. 6b), suggesting that the above-observed effects of BafA1 on intracellular Bac genome were unlikely due to its side effects on cells. Collectively, these data established a link between NPC1-mediated endosomal escape and the exposure and decay of Bac genome in cytoplasm.

EXTL3 participates in baculovirus entry through heparan sulfate biosynthesis pathway

EXTL3 (Exostosin-like protein 3) belongs to EXT protein family, which includes EXT1, EXT2, EXTL1, EXTL2, and EXTL3[73]. *EXTL3* encodes a glycosyltransferase responsible for the biosynthesis of heparan sulfate (HS). Two glycosyltransferase domains, GT47 and GT64, of EXTL3 in the Golgi luminal region are the functional domains for HS biosynthesis[74] (Fig. 3a). We constructed *EXTL3*$^{-/-}$ HEK-293T cells (Supplementary Fig. 7a) to explore the function of EXTL3-mediated HS biosynthesis in baculovirus transduction. It was found that baculovirus attachment and entry in *EXTL3*$^{-/-}$ cells were markedly reduced as compared to non-targeting sgRNA cells (Fig. 3b). These results were consistent with those in HeLa cells and illustrated an important role of EXTL3 in baculovirus attachment and entry.

Given that HS is a known baculovirus attachment and entry factor in mammalian cells[54–56], we sought to explore whether EXTL3 affected baculovirus attachment and entry by affecting HS biosynthesis. We thus examined the expression of heparan sulfate proteoglycan 2 (HSPG2) protein in *EXTL3*$^{-/-}$ HEK-293T cells and found that *EXTL3* knockout abolished the production of HSPG2 (Fig. 3c). In addition, we found that Bac-EGFP transduction could be inhibited by heparin sodium in a dose-dependent manner (Fig. 3d and Supplementary Fig. 7b), which is a competitive inhibitor for cellular HS[65,75]. Similarly, 2 μg/μL heparin sodium could significantly inhibit baculovirus attachment and entry (Fig. 3e). Moreover, 24 h pretreatment with heparanase (HPSE) could significantly reduce baculovirus transduction in non-targeting sgRNA control cells or in overexpression-rescued *EXTL3*$^{-/-}$ cells (Fig. 3f). These results collectively suggested that HS was important for baculovirus attachment and entry and that EXTL3 promoted baculovirus transduction by involving in HS biosynthesis.

Next, we sought to investigate whether other members in the EXT protein family have similar roles in baculovirus transduction. HS biosynthesis is initiated by the attachment of xylose to specific serine residues in HSPG core proteins, followed by the formation of a linkage tetrasaccharide, glucuronic acid-galactose-galactose-xylose (GlcA-Gal-Gal-Xyl). EXTL3 links the first N-acetyl-D-glucosamine (GlcNAc) residue to GlcA and an enzyme complex composed of EXT1 and EXT2 adds GlcA-GlcNAc disaccharide repeats to the nascent chain, followed by a series of processing reactions[76] on the chain (Fig. 3g). We constructed *EXT2* knockout HEK-293T cells (Supplementary Fig. 7c) and found that *EXT2* knockout could also affect baculovirus transduction (Fig. 3h) though the degree of inhibition was not as prominent as those with *EXTL3* knockout. These results suggested that different moieties or forms of HSPG may have differential effects on baculovirus transduction.

Next, we sought to explore the relationship between EXTL3 and NPC1 functions in baculovirus transduction. We found that in the presence of heparin sodium, the efficiency of baculovirus transduction in *NPC1*$^{-/-}$ HeLa cells was further reduced (Fig. 3i and Supplementary Fig. 7d). In addition, *NPC1* overexpression rescue did not eliminate the inhibitory activity of heparin sodium on baculovirus transduction (Fig. 3i and Supplementary Fig. 7d). These results suggested that NPC1 could affect baculovirus transduction through a EXTL3-independent pathway and that the functions of NPC1 and EXTL3 in baculovirus transduction were additive to each other.

NPC1 participates in baculovirus endosomal escape mainly through I and C domain-mediated membrane fusion

To elucidate the mechanism of action of NPC1 in baculovirus endosomal escape, we first used DiOC18 dye to label baculovirus particles (DiOC18-Bac-EGFP). The fluorescence of DiOC18 is self-quenched in labeled viruses and dequenched when membrane fusion occurs[77,78]. DiOC18-staining experiments showed that the membrane fusion of baculovirus was significantly suppressed in *NPC1*$^{-/-}$ HeLa cells which could be restored by *NPC1* overexpression, as analyzed by confocal microscopy and flow cytometry experiments (Fig. 4a, b). These results are consistent with the above findings and strongly suggested that NPC1 promoted baculovirus endosomal escape by involving in membrane fusion.

NPC1 contains 13 transmembrane helices (TM) and 3 distinct lumenal domains A, C, and I[79] (Fig. 4c). It has been reported that NPC1 affects the endosomal escape of Ebola virus through its C domain[67,80]. To assess which luminal domain of NPC1 interacts with GP64, we performed co-immunoprecipitation experiments. We designed constructs encoding individual domains of A, C, and I (NPC1-A, NPC1-C, and NPC1-I), and constructs with deletions of individual domain (NPC1-ΔA, NPC1-ΔC, and NPC1-ΔI) (Fig. 4d). Co-IP analyses of the interactions between GP64 and NPC1-A, NPC1-C or NPC1-I showed that both NPC1-C and NPC1-I could interact with GP64 (Fig. 4e). Additional Co-IP analyses showed that GP64 could interact with full-length NPC1 and truncation constructs NPC1-ΔA, NPC1-ΔC and NPC1-ΔI (Fig. 4f), suggesting that the A, C or I domains might have redundant functions for GP64 binding. Collectively, these Co-IP experiments suggested that the C and I domains of NPC1 could both involve in the interactions with GP64.

To understand the roles of individual NPC1 domains in supporting baculovirus transduction, we performed a rescue experiment by

https://doi.org/10.1038/s41467-024-52193-w

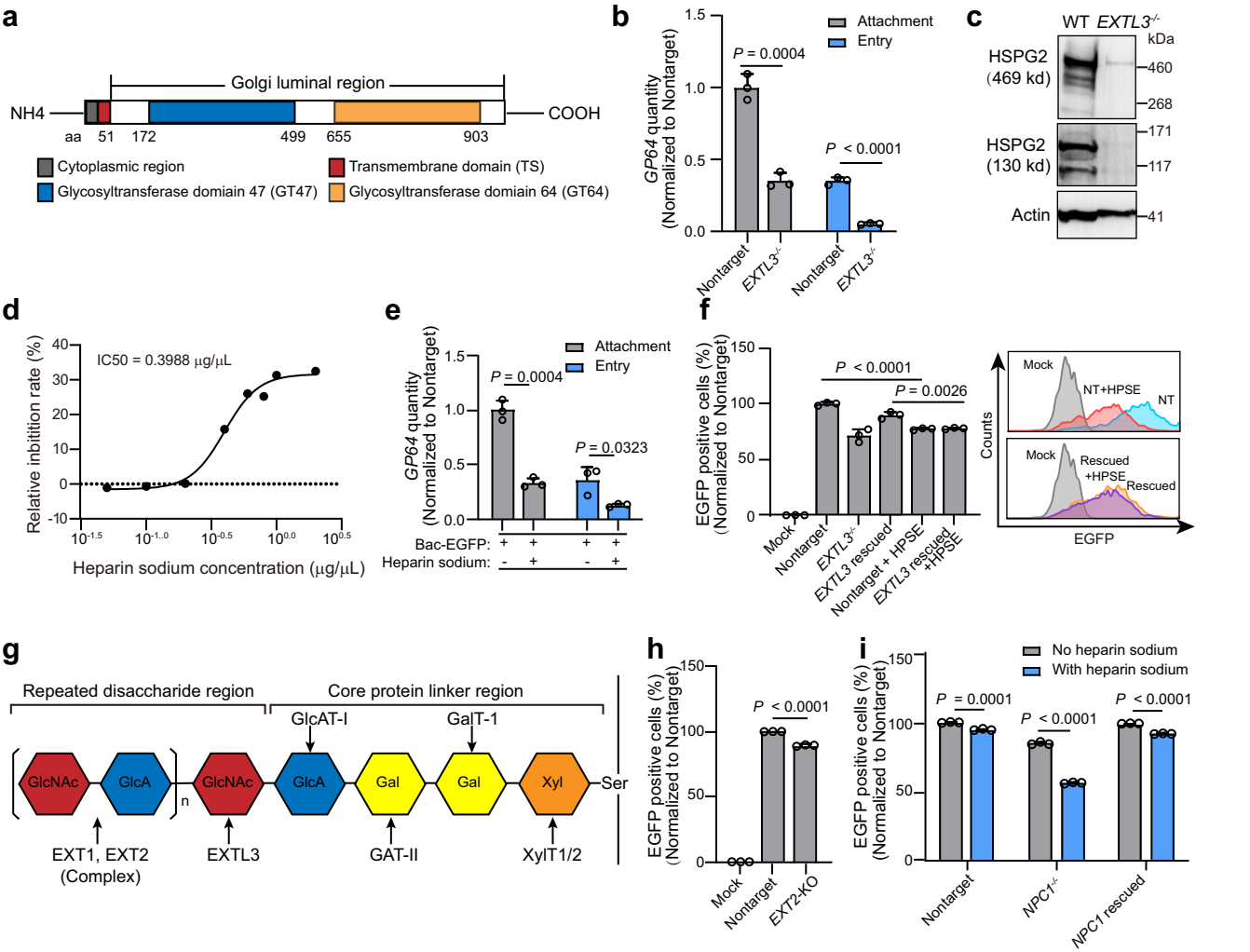

Fig. 3 | Investigation of the functions of EXTL3-mediated heparin biosynthesis in baculovirus transduction in HEK-293T cells. a Structural organization of EXTL3 protein. **b** Evaluation of baculovirus attachment and entry in *EXTL3*$^{-/-}$ cells. *GP64* gene was quantified by qPCR. The *p*-value between Nontarget and *EXTL3*$^{-/-}$ in entry groups is 4e-5. **c** Western blotting detection of heparan sulfate proteoglycan 2 (HSPG2) in wild-type and *EXTL3*$^{-/-}$ cells. The experiment is repeated three times independently with similar results. **d** Analysis of the effects of heparin sodium on Bac-EGFP transduction, as determined by flow cytometry quantification of EGFP-positive cells. **e** Analysis of the effects of heparin sodium on Bac-EGFP attachment and entry, as determined by qPCR quantification of attached or internalized baculovirus *GP64* gene. **f** Evaluation of the effects of HPSE on baculovirus transduction. The *p*-value between Nontarget and Nontarget+HPSE groups is 2e-5. **g** Schematic presentation of HSPG biosynthesis. **h** Evaluation of the effects of *EXT2* knockout on baculovirus transduction. The *p*-value between Nontarget and *EXT2*-KO groups is 7e-6. **i** Investigation of the relationship between EXTL3 and NPC1 functions in baculovirus transduction. The *p*-value between No heparin sodium and With heparin sodium in *NPC1*$^{-/-}$ groups is 1e-6. The *p*-value between No heparin sodium and With heparin sodium in *NPC1* rescued groups is 2e-6. For (**b**, **e**, **f**, **h**, and **i**), Data are presented as mean ± SD ($n = 3$) from three biological replicates. The significant difference is analyzed by two-tailed unpaired Student's *t*-test. Mock group is the PBS treatment without baculovirus. Source data are provided as a Source Data file.

generating stable cell lines harboring full-length NPC1 or truncation constructs on the basis of *NPC1*$^{-/-}$ HeLa cells (Supplementary Fig. 8a). It was found that the truncation construct NPC1-ΔA could partly restore the susceptibility of cells to baculovirus transduction whereas NPC1-ΔC or NPC1-ΔI did not significantly restore baculovirus transduction (Fig. 4g and Supplementary Fig. 8b). These results were consistent with the Co-IP results in that C and I domains play more important roles in baculovirus transduction than A domain. In addition, we noted that while full-length NPC1 could restore baculovirus transduction to a level similar to that in non-targeting sgRNA group, none of the truncation constructs could achieve a comparable rescuing efficiency (Fig. 4g). This suggested that the intact structural organization of NPC1 could be important for GP64 binding and baculovirus transduction. Collectively, the above results suggested that C and I domains played predominant roles in NPC1 binding with GP64 while the intact structure of NPC1 might be also important.

Next, we sought to investigate whether purified proteins of NPC1 C and I domains could interact with baculovirus or baculovirus proteins. We first performed a neutralization experiment with a commercial recombinant protein of NPC1 C domain (residues R372 to F622). It was found that NPC1 C domain could inhibit Bac-EGFP transduction in a dose-dependent manner in HEK-293T cells (Fig. 4h). Because the function of NPC1-I domain was rarely reported in viral infection and no commercial source could be found, we expressed and purified GST tagged NPC1-I domain protein from BL21 (DE3) Escherichia coli cells. Despite of an unknown impurity band (Supplementary Fig. 8c), the identity of the target protein band was confirmed by mass spectrometry (Fig. 4i). We set a far WB assay to investigate the interaction between NPC-I and GP64, where GST-tagged NPC1-I domain was resolved by SDS-PAGE, transferred to a PVDF membrane and then probed with purified GP64 protein. It was found that NPC1-I domain could directly interact with GP64 in vitro (Fig. 4j). Interestingly, we

https://doi.org/10.1038/s41467-024-52193-w

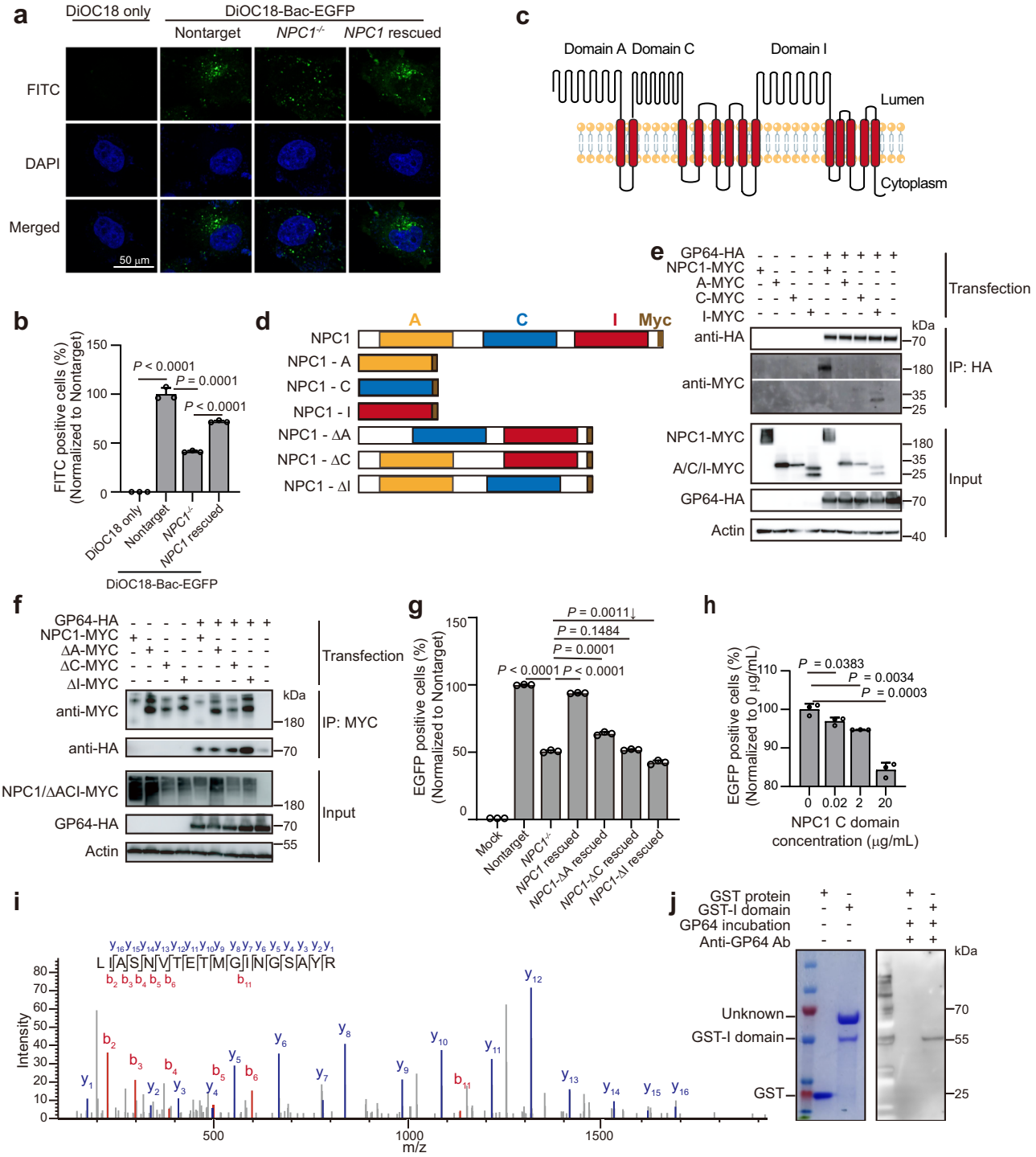

Fig. 4 | Dissection of the function of NPC1 in baculovirus endosomal escape. DiOC18-staining experiment for illustration of NPC1 function in baculovirus membrane fusion, as analyzed by confocal microscopy (**a**) or flow cytometry analyses (**b**). The *p*-value between DiOC18 only and Nontarget groups is 1e-5. The *p*-value between *NPC1*$^{-/-}$ and *NPC1* rescued groups is 4e-6. **c** The structural organization of NPC1. **d** Design of NPC1 constructs. Analyses of the interactions between HA-tagged GP64 and Myc-tagged full-length NPC1, NPC1-A, NPC1-C, NPC1-I (**e**), NPC1-ΔA, NPC1-ΔC or NPC1-ΔI (**f**). **g** Investigation of the effects of overexpression rescue with full-length or truncation constructs of NPC1 on baculovirus transduction, as determined by the EGFP-positive cells via flow cytometry. Mock, PBS treatment without baculovirus. The *p*-values between *NPC1*$^{-/-}$ and Nontarget and *NPC1* rescued groups are 8e-8 and 1e-7, respectively. **h** Neutralization of Bac-EGFP transduction in HEK-293T cells by recombinant protein of NPC1 C domain, as determined by flow cytometry analyses. **i** ESI-MS confirmation of purified GST-I protein ($n = 1$). **j** Far-western analysis of the interaction between GP64 and GST-I. For (**b**, **g**, and **h**), Data are presented as mean ± SD ($n = 3$) from three biological replicates. The significant difference is analyzed by two-tailed unpaired Student's *t*-test. For (**e**, **f**, and **j**), The experiment is repeated three times independently with similar results. Source data are provided as a Source Data file.

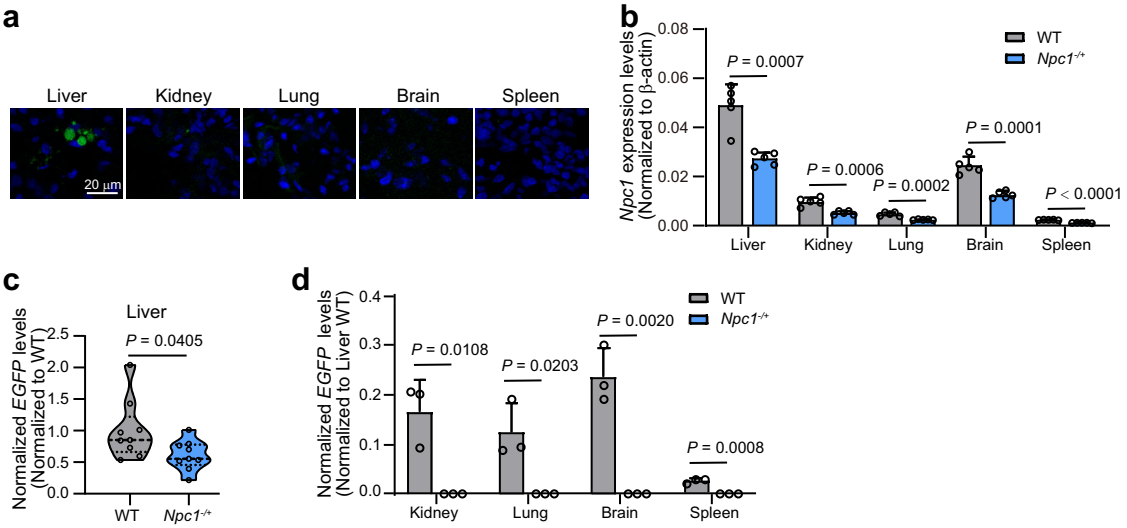

Fig. 5 | Baculovirus transduction in mouse liver is dependent on NPC1. **a** Investigation of the tissue tropism of Bac-EGFP in wild-type mice at 72 h post intravenous injection, as determined by EGFP expression at protein ($n = 3$). The fluorescence images are acquired using confocal microscopy on flash-frozen tissues that are fixed with optimal cutting temperature compound (OCT). **b** RT-qPCR quantification of *NPC1* mRNA in the lysate of liver, kidney, lung, brain, and spleen in wild-type and *Npc1*$^{-/+}$ mice. The *p*-value between WT and *Npc1*$^{-/+}$ in spleen groups is 1e-8. RT-qPCR quantification of *EGFP* mRNA in the lysate of liver (**c**) and other tissues including kidney, lung, brain, and spleen (**d**) in wild-type and heterozygous *Npc1*$^{-/+}$ knockout mice at 72 h post-Bac-EGFP injection. The *EGFP* mRNA in the lysates of kidney, lung, brain, and spleen (**d**) in heterozygous *Npc1*$^{-/+}$ knockout mice is below the limit of detection. For (**b**–**d**), β-actin is used as an internal control. The data in this figure are from independent biological replicates. The significant difference is analyzed by two-tailed unpaired Student's *t*-test. For (**b** and **d**), Data are presented as mean ± SD of biological replicates ($n = 5$ for (**b**) and = 3 for (**d**)). For **c**, Data are collected from nine biological replicates ($n = 9$). The thick horizontal dashed line represents the median and thin horizontal dashed line indicates interquartile range between 25th and 75th percentile. Source data are provided as a Source Data file.

found that NPC1-C and NPC1-I shared 30% protein sequence similarity as analyzed by ClustalW (Supplementary Fig. 8d). It was thus likely that NPC1-I resembled NPC1-C for virus interaction and endosomal escape, as reported in Ebola virus[67,80,81].

Baculovirus transduction in mouse liver is dependent on NPC1

To understand baculovirus transduction in mice, we first examined the toxicity of intravenously administrated baculovirus. We administrated Bac-EGFP to C57BL/6J mice via tail vein and found that Bac-EGFP resulted in a transient loss of body weight in the first four days post injection (Supplementary Fig. 9a), which was eventually recovered. Similarly, a transient change of blood routine was observed in Bac-EGFP-treated mice (Supplementary Fig. 9b).

We then analyzed the vulnerability of different tissues to baculovirus transduction in wild-type mice and found that liver displayed highest degree of Bac-EGFP transduction (Fig. 5a, d). It was noted that wild-type mice liver exhibited highest expression of *Npc1* (Fig. 5b). To investigate whether baculovirus transduction in mouse liver was related with *Npc1* expression, we sought to construct *Npc1* knockout mice. Unfortunately, *Npc1*$^{-/-}$ C57BL/6J mice showed notably reduced birth rate and body weight (Supplementary Fig. 9c). A previous study also showed that homozygous *Npc1* knockout in mice resulted in reduced general health and pathologic changes in multiple organs[82]. By contrast, *Npc1*$^{-/+}$ mice did not show defects in birth rate or body weight (Supplementary Fig. 9c), nor did liver show pathologic changes as compared to wild-type mice (Supplementary Fig. 9d). Therefore, we used *Npc1*$^{-/+}$ heterozygous C57BL/6J mice for subsequent analyses. The gene disruption of *Npc1* was validated in the mRNA levels (Fig. 5b). Importantly, Bac-EGFP transduction in liver tissues of *Npc1*$^{-/+}$ mice was significantly reduced (Fig. 5c) as compared to that in wild-type mice,-suggesting that baculovirus transduction in mouse liver was dependent on *Npc1* expression. It was also noted that in *Npc1*$^{-/+}$ mice, *EGFP* mRNA could not be detected in organs other than liver (Fig. 5d).

Discussion

The large packaging capacity allows baculovirus to carry multiple transgene cassettes for the expression of large protein complexes in insect cells[83–85]. For the same reason, baculovirus has been an attractive gene therapy vector for delivering large or multiple gene cassettes in single viral particles, which can overcome the packaging limitation associated with conventional viral vectors. However, despite of the existing studies on baculovirus entry mechanism in mammalian cells[54,55,57–59], there has been no systematic investigation on baculovirus host factors in mammalian cells. In the present study, we performed a forward genetic screen using the SfCRISPR library that carries approximately 1400 cell surface proteins. Two proteins, EXTL3 and NPC1, were identified as host dependency factors and were shown to involve in baculovirus attachment and entry, and endosomal escape processes respectively.

Investigation of EXTL3 suggested that it promoted baculovirus attachment and entry by mediating heparan sulfate (HS) biosynthesis. EXT2, another enzyme involved in HSPG biosynthesis, was also shown to affect baculovirus transduction. These results were consistent with the previous findings[54,55] and confirmed the importance of HS for baculovirus transduction. As HS is widely distributed across different cell types and tissues, we did not further explore the dependency of baculovirus transduction on HS. However, it is likely that different cells or tissues display different expression profiles of EXT family proteins or proteins related to HS biosynthesis, which can be important determinants for baculovirus transduction.

Moreover, it was found in the present study that NPC1 participated in baculovirus membrane fusion and endosomal escape, but not entry or attachment. These findings were consistent with the function of NPC1 in infection of filoviruses[86] and African swine fever virus (ASFV)[87]. Unlike the case in EBOV where the C domain of NPC1 interacted with EBOV glycoprotein[86], it was found in the present study that both the C and I domains of NPC1 interacted with baculovirus GP64 protein. Additionally, an NPC1 inhibitor U18666A that can block EBOV

infection was found to be efficient in inhibiting baculovirus transduction in mammalian cells. The structural basis of baculovirus GP64 interaction with NPC1-C and -I domains and the mechanism of U18666A-mediated inhibition of baculovirus transduction require further investigation. In consistency with these observations in mammalian cells, previous studies suggested that *Bombyx mori* NPC1 and NPC2 proteins promoted *Bombyx mori* nucleopolyhedrovirus (BmNPV) infection in insect cells by facilitating membrane fusion and endosomal escape[88,89]. More interestingly, BafA1 treatment experiments suggested the NPC1-mediated endosomal escape could release Bac genome into cytoplasm for transgene expression, the process of which will also accelerate Bac genome degradation.

One major discovery in the present study is that partial knockout of *Npc1* reduced baculovirus transduction in mouse liver. To the best of our knowledge, this was the first study revealing host factors for in vivo baculovirus transduction in mammals. This result implied that the expression of NPC1 and its function in endosomal escape could be a critical determinant for baculovirus transduction in mammals. This knowledge can be exploited to design novel strategies of targeted baculovirus delivery for tissues or cells with high NPC1 expression. In addition, our study shed light on engineering baculovirus GP64 protein for enhanced interactions with mammalian NPC1. Nevertheless, although the present and previous studies revealed general safety of baculovirus administration in mice, the safety of baculovirus in humans remains unknown and should be carefully addressed in future studies.

In addition to *EXTL3* and *NPC1*, our studies revealed several other genes that might involve in baculovirus transduction in HEK-293T cells. Among these genes, *MBTPS2* seemed to have a major impact on the transduction efficiency. *MBTPS2* encodes site-2 protease (S2P), which is a hydrophobic zinc metalloprotease. S2P can cleave transmembrane proteins to release their nucleus-localizing components that regulate the transcription of genes involved in lipid biosynthesis[90] and ER stress response[91]. It has been reported that S2P can mediate the activation of antiviral proteins through regulated intramembrane proteolysis (RIP) process during HCV infection[92]. Thus, it could be interesting to investigate in future studies whether MBTPS2 plays similar functions during baculovirus transduction in mammalian cells.

One limitation in our study was that the HEK-293T cells used in the screening process were deficient of cyclic GMP-AMP synthase-stimulator of interferon genes (cGAS-STING) pathway. While the high baculovirus transduction efficiency in HEK-293T could reduce the background signal in the negative EGFP selection, the lack of cGAS-STING pathway eliminated the possibility of uncovering host factors involved in cGAS-STING signaling Recent studies showed that cGAS-STING signaling could impede baculovirus transduction in mammalian cells by affecting interferon (IFN) production[60]. Interestingly, cGAS-STING-mediated IFN production in mammalian cells could be inhibited by AcMNPV P26 protein[93]. In future studies, it would be interesting to perform CRISPR screen on cGAS-STING-competent cells to uncover baculovirus host factors that act in the context of IFN signaling.

Methods

Cell culture

HeLa cells were obtained from the American Type Culture Collection (ATCC). HEK-293T, U87-MG, Club, HK-2, U251, and A549 cells were obtained from the Cell Bank of Shanghai Institutes for Biological Science (SIBS). All the cells used in this study were validated by VivaCell Biosciences (Shanghai, China). All cells were grown in Dulbecco's modified Eagle's medium (DMEM, Thermo, Pittsburgh, USA) supplemented with 10% fetal bovine serum (FBS, Thermo) and 1% penicillin-streptomycin (Thermo) and maintained at 37 °C in a fully humidified incubator containing 5% CO_2. All cells were confirmed by PCR to be free of mycoplasma contamination.

Lentivirus production and transduction

To produce lentivirus (LVs), HEK-293T cells at a confluence of 70–90% were transfected with LV packaging plasmid pMD2.G, envelope plasmid psPAX, and transfer plasmid pLentiCRISPR-v2 that carried Cas9 gene and a single sgRNA or pooled sgRNA plasmid library with a mass ratio of 1: 1.5: 2 using Lipofectamine 3000 (Thermo). In the case of overexpression, the transfer plasmids were pLenti-EF1α-IRES-NPC1-Bsd, plenti-EF1α-IRES-EXTL3-Bsd, pLenti-EF1α-IRES-NPC1ΔA-Bsd, pLenti-EF1α-IRES-NPC1ΔC-Bsd and pLenti-EF1α-IRES-NPC1ΔI-Bsd). At 6 h after transfection, the medium was replaced with fresh medium. The medium supernatant containing LVs was harvested at 48–60 h post-transfection by centrifugation at 2000 rpm (420 × *g*) for 10 min, filtrated through a 0.45 μm filter (Merck, Darmstadt, Germany) and stored at −80 °C.

HeLa cells and HEK-293T cells were transduced with LVs in the presence of polybrene (10 μg/mL, Merck) using spinfection through centrifugation at 2000 rpm (420 × *g*) for 2 h. At 24 h post-transduction, LV-containing medium was removed and cells were cultured in fresh medium in the presence of 1–2 μg/mL puromycin for 3 to 5 days or 2–5 μg/mL blasticidin (Thermo) for 7–10 days to remove empty cells containing no LVs. Finally, survived cells were collected, aliquoted, and stored in liquid nitrogen.

Baculovirus production and transduction

Bac-EGFP recombinant viruses were generated using Bac-to-Bac baculoviral expression system (Thermo, Cat. No. A11101). Transgene plasmid pFastBac carrying *EGFP* gene was transformed into DH10Bac E. coli competent cells that harbored the parental bacmid to form a recombinant bacmid encoding the *EGFP* transgene. The recombinant bacmid was then transfected into insect cells for production of recombinant baculovirus particles. At 72 h post-transfection, the culture supernatant containing baculovirus particles was harvested and concentrated by Optima XPN-100 Ultracentrifuge (Beckman Coulter, California, USA). Virus titer was determined using the 50% tissue culture infectious dose ($TCID_{50}$) assay[94].

For baculovirus transduction, HEK-293T or HeLa cells were seeded at a cell density of 40%. At 24 h after seeding, the cells were transduced with baculovirus at an MOI of 1 or 2 for HEK-293T or HeLa respectively. MOIs other than 1 and 2 were indicated in figure legends. At 24 h after baculovirus transduction, baculovirus-containing medium was removed and the cells were incubated in DMEM (Thermo) supplemented with 10% FBS (Thermo) for another 24 h. Thereafter, the cells were collected and the efficiency of baculovirus transduction was quantified by flow cytometry (CytoFLEX, Beckman Coulter, California, USA) and visualized by fluorescence microscope (EVOS M5000, Thermo). The expression of *EGFP* mRNA was quantified by RT-qPCR using specific primers (Supplementary Table 2).

Construction of surfaceome CRISPR library

The human surfaceome CRISPR library was described in our previous work[62], which contained 16,975 sgRNAs targeting 1314 surface protein genes and 1000 non-targeting sgRNAs. To construct surfaceome CRISPR library in HEK-293T, the cells were transduced with LV library at an MOI of 0.3 using spinfection as described above. Cells of more than 500-fold coverage of the library size were collected, aliquoted, and stored in liquid nitrogen.

CRISPR screening for baculovirus host factors and next-generation sequencing (NGS) analyses of sgRNA enrichment

The HEK-293T cell library of 1×10^7 cells was seeded onto 15 cm petri dishes. At 24 h after seeding, the cells were incubated with recombinant baculovirus carrying an *EGFP* transgene (Bac-EGFP) of 3×10^7 infective units (IU) for 24 h. The medium containing virus was then removed and cells washed with phosphate-buffered saline (PBS) for three times and then cultured in fresh medium for

another 24 h. Then the treated cells were harvested and sorted using flow cytometry (Moflo, Beckman Coulter, California, USA) for EGFP-negative cells. Genomic DNA of the sorted cells was extracted using phenol: chloroform: isoamyl alcohol (v/v/v, 25:24:1) and then purified using ethanol precipitation. Genome-integrated sgRNAs were amplified from the collected genomic DNA by PCR using primers containing Illumina adapters (Supplementary Table 1). PCR amplicons were analyzed by Genewiz (Suzhou, Jiangsu, China) using next-generation sequencing (NGS) on Illumina HiSeq 3000 platform. After removing the adapters, the 20 bp sgRNA was mapped to the reference sgRNA with 1 bp mismatch allowed. The raw read counts were subjected to MAGeCK analyses to determine the enriched sgRNA and gene knockouts. A false discovery rate (FDR) of less than 0.05 was applied to identify significantly enriched sgRNAs and candidate gene knockouts.

Generation of gene knockout cells

The LV transfer plasmids pLentiCRISPR-v2-sgRNA carrying single sgRNAs (Supplementary Table 3) for knockout cell line construction were generated as previously described above[62]. The LVs were packaged and transduced onto cells as described above. To evaluate the knockout efficiency, the genomic DNA of knockout cells was extracted using Quick Extraction kit (Lucigen, Wisconsin, USA) and the modified genomic sites were PCR amplified using corresponding primers (Supplementary Table 4). The PCR amplicons were sequenced by Sanger sequencing (Genewiz) and gene disruption efficiency was analyzed by TIDE website (https://tide.nki.nl/)[95]. Single clones were obtained by cell sorting using flow cytometry (Moflo, Beckman) and genotyped by Sanger sequencing to determine the mutations at each allele.

RT-qPCR

Total RNA from cultured cells was extracted using TRIzol (Thermo), chloroform (Sinopharm, Ningbo, China) and purified using isopropanol precipitation. RNA was then reverse transcribed into cDNA by PrimeScript RT reagent Kit with gDNA Eraser (Takara Bio Inc., Shiga, Japan). The mRNA levels were determined by reverse transcription quantitative PCR (RT-qPCR) using SYBR green dye on Applied Biosystems Q6 Real-Time PCR cycler (Thermo) and specific primers (Supplementary Table 2). All SYBR Green primers were validated with dissociation curves. The expression of genes was normalized to β-actin or *RPLP0*.

For RT-qPCR on mouse tissues, the tissue samples were collected, frozen in liquid nitrogen, and homogenized using grinding beads through tissue grinding device (Jingxin, Shanghai, China) in TRIzol reagent (Thermo). The extraction and quantification processes in tissue RNA were the same to that in cell culture samples as described above.

qPCR quantification of baculovirus genome

Genomic DNA of baculovirus or baculovirus-containing cells was extracted using phenol: chloroform: isoamyl alcohol (v/v/v, 25: 24: 1) and then purified using ethanol precipitation. The total DNA concentration was determined for each sample. For quantitative PCR (qPCR) reaction, 2 ng total DNA was added into each reaction as the template. *GP64* DNA, which was used as indicator of viral genome content, was quantified by qPCR using SYBR green dye on Applied Biosystems Q6 Real-Time PCR cycler (Thermo) and specific primers (Supplementary Table 2). All SYBR Green primers were validated with dissociation curves. The genomic DNA level was normalized to β-actin.

Gene knockdown using siRNA

HEK-293T cells were seeded onto 6-well plates with a density of 5×10^5 cells per well. At 24 h after seeding, cells were transfected with 100 pmol siRNA (Genepharma, Shanghai, China) (Supplementary Table 5) using 7.5 μL Lipofectamine 2000 (Thermo) for 6 h, then washed with PBS and cultured in fresh DMEM (Thermo) supplemented with 10% fetal bovine serum (FBS, Thermo). At 48 h post-transfection, cells were infected with baculovirus at an MOI of 1 for 24 h, then washed with PBS for three times and cultured in fresh medium for 24 h. The cell samples were harvested and lysed for total RNA extraction, and the mRNA levels of *EGFP*, *EXTL3*, and *NPC1* in cell lysate were determined using RT-qPCR as described above.

Virus attachment and entry assays

Virus attachment and entry assays were performed as described[96] with minor modifications. HEK-293T cells or HeLa cells were seeded onto 12-well plates at a density of 200,000 cells per well and incubated overnight. For virus attachment assay, cells were incubated with baculovirus at an MOI of 20 in cold medium without FBS on ice for 60 min, then washed with cold Dulbecco's phosphate-buffered saline (DPBS) for three times and harvested. The baculovirus genomic DNA was extracted from the cells containing attached virus and quantified by qPCR as described above. For virus entry assay, cells were incubated with baculovirus at an MOI of 20 in cold medium on ice for 60 min, washed by cold DPBS for three times, treated with pre-warmed medium containing FBS, and then incubated at 37 °C for 40 min. The treated cells were washed with PBS for three times and then treated with 0.25% trypsin (Thermo) for 30 s to remove surface-bound baculovirus particles. The genomic DNA of internalized baculovirus was extracted and quantified by qPCR as described above.

Construction of stable cell lines harboring overexpressed genes

EXTL3 and *NPC1* genes were codon-optimized for expression in human cells and synthesized by Genewiz (Supplementary Tables 6, 7). The 20 bp sgRNA-targeting sites and PAM sequences were mutated with silent mutations. Myc and FLAG tags were added to the C-terminus of these genes for WB detection. These genes were cloned into the XbaI and BamH1 sites of pLV-EF1α-IRES-Bsd plasmid. The lentiviral overexpression plasmids of NPC1 truncation mutants (NPC1-ΔA, NPC1-ΔC, and NPC1-ΔI) were constructed from the full-length gene in pLV-EF1α-IRES-NPC1-Bsd. For LV packaging, the transgene plasmid containing EXTL3, NPC1, NPC1ΔA, NPC1ΔC or NPC1ΔI was co-transfected into HEK-293T cells with helper plasmids pMD2.G and psPAX as described above. The transgene-containing LVs were transduced into *EXTL3*$^{-/-}$ or *NPC1*$^{-/-}$ cells, and the cells were subjected to selection with 2 μg/mL blasticidin (Thermo) for 7 to 10 days to purge empty cells containing no LVs. Finally, survived cells were collected, aliquoted, and stored in liquid nitrogen.

Analysis of the intracellular baculovirus genomic DNA

The experiment was performed in an approach similar to a previous study[62]. Non-targeting sgRNA-treated, *NPC1*$^{-/-}$ and *NPC1* overexpression rescued HeLa cells were seeded onto 24-well plates at a density of 80,000 cells per well and incubated overnight. The next day the cells were incubated with Bac-EGFP at an MOI of 2 for 1 h. The virus-containing medium was removed and the cells were washed with PBS for three times and then treated with 0.25% trypsin (Thermo) for 30 s to remove surface-bound baculovirus particles. These treated cells were supplemented with pre-warmed DMEM medium containing FBS and then incubated at 37 °C for indicated time. Intracellular baculovirus genomic DNA was extracted from each well. The total baculovirus *GP64* amount in each well was determined by qPCR and then normalized to the zero time point.

Cell Counting Kit-8 assay (CCK-8)

Non-targeting sgRNA, *NPC1*$^{-/-}$, and *NPC1* rescued HeLa cells were seeded onto 96-well plates at a density of 10,000 cells per well and incubated at 37 °C overnight. The cells were incubated with Bac-EGFP

at an MOI of 2 for 1 h, washed with PBS for three times and then treated with 0.25% trypsin (Thermo) for 30 s to remove surface-bound baculovirus particles. At indicated time points, the supernatant was removed and cells incubated with complete medium containing 10% CCK-8 reagent (MeilunBio, Liaoning, China) at 37 °C for 1 h. Cell proliferation was quantified by measuring absorbance at 450 nm using microplate reader (SpectraMax iD3, Molecular Devices, Shanghai, China). The background signal in empty wells without cells was subtracted from each sample.

Bafilomycin A1 (BafA1) treatment

Wild-type HeLa cells were seeded on to 24-well plates at a density of 80,000 cells per well and incubated overnight. The next day the cells were pre-incubated with 100 nM BafA1 (MedChemExpress, New Jersey, USA, Cat. No. HY-100558) for 1 h, followed by transduction with Bac-EGFP at an MOI of 2 for 1 h in the presence of 100 nM BafA1. The virus-containing medium was then removed, the cells washed three times with PBS and then treated with 0.25% trypsin (Thermo) for 30 s to remove surface-bound baculovirus particles. These cells were incubated in DMEM medium containing FBS and 10 nM BafA1 for indicated time. The genomic DNA of intracellular baculovirus was extracted from cells and quantified by qPCR as described above.

For CCK-8 assay, cells were seeded on to 96-well plates at a density of 10,000 cells per well. The next day, the cells were pre-incubated with 100 nM BafA1 and transduced with Bac-EGFP to mimic the treatment as described above. At 48 h after removal of virus, cell proliferation was quantified by CCK-8 as described above at indicated time points.

WB analyses

For WB analyses, cells were lysed with RIPA buffer (Beyotime Biotechnology, Beijing, China) on ice for 10 min and centrifuged at 12,000 rpm (13,523 × *g*) at 4 °C for 10 min to remove cell debris. The total protein concentration in cell lysate was determined using the BCA Protein Assay Kit (Thermo). Cell lysate was mixed with SDS-PAGE loading buffer (Takara) containing 200 mM dithiothreitol (DTT), incubated at 95 °C for 10 min, and resolved on 4–12% PAGE gels (GenScript, Nanjing, China). Protein samples were transferred onto nitrocellulose membranes (Merck) using an iBlot gel transfer system (Thermo). The following primary and secondary antibodies were used in WB including anti-Myc rabbit antibody (CST, Cat. No. 2272S), anti-HA rabbit antibody (CST, Cat. No. 3724S), anti-Heparan Sulfate Proteoglycan 2/Perlecan antibody (Abcam, Cambridge, UK, Cat. No. ab255829) and HRP-conjugated anti-rabbit IgG (CST, Cat. No. 5127S). Anti-β actin antibody conjugated with HRP (CST, Cat. No. 5125S) was used as an internal control.

Co-immunoprecipitation (Co-IP)

HEK-293T cells were seeded onto 6-well plates at a density of 1×10^6 cells per well. After the confluency reached 70% to 80%, plasmid was transfected into cells. Plasmids containing Myc-labeled NPC1 or NPC1 mutant and plasmids containing HA-labeled GP64 (Supplementary Table 8) were co-transfected into HEK-293T cells by Lipofectamine 3000 (Thermo). At 24 h after transfection, cells were resuspended with co-IP lysis buffer. One-half of the lysate was used to incubate with magnetic beads (Thermo) containing anti-HA or anti-Myc antibodies at room temperature for 1 h. Magnetic beads were collected with a magnetic rack (Thermo), then proteins bound to the magnetic beads were eluted by 1x SDS-PAGE loading buffer containing DTT. Finally, total proteins and co-immunoprecipitated proteins were detected by WB as described above.

Recombinant NPC1 protein neutralization assay

HEK-293T cells were seeded on to 48-well plates at a density of 1×10^5 cells per well. After Bac-EGFP incubation with recombinant protein of NPC1 C domain (residues R372-F622) (SinoBiological, Beijing, China, Cat. No. 16499-H32H) at indicated concentrations at 4 °C for 30 min. Thereafter, HEK-293T cells were transduced with Bac-EGFP at an MOI of 1 for 24 h in the presence of NPC1-C domain protein. Then baculovirus-containing medium was removed and the cells were incubated in DMEM (Thermo) supplemented with 10% FBS (Thermo) for 24 h and then harvested. The efficiency of baculovirus transduction was quantified by flow cytometry (CytoFLEX, Beckman Coulter, California, USA).

Expression and purification of the human NPC1-I domain

NPC1-I domain was codon-optimized for expression in Escherichia coli, synthesized by Genewiz, and cloned into pGEX4T-1-GST plasmid. The recombinant pGEX4T-1-GST-NPC1-I plasmid was transformed into chemically competent BL21 (DE3) E. coli cells. After overnight culturing, single colonies were selected and amplified in Luria–Bertani (LB) medium containing (100 mg/mL) ampicillin overnight. The next day, the culture was inoculated into fresh LB medium at 1: 100 dilution and cultured at 37 °C for about 3 h until OD_{600} reached 0.6–0.8. Protein expression was induced with 0.5 mM isopropyl β-D-thiogalactoside (IPTG) at 22 °C overnight. The cells were then collected by centrifugation at 4,000 rpm (1681 × *g*) for 15 min at 4 °C.

For protein purification, the cell pellet was resuspended with PBS and then lysed by sonication. The cell lysate was centrifuged at 12,000 rpm (13,523 × *g*) for 30 min at 4 °C and the supernatant was isolated. The supernatant was run through a glutathione resin affinity chromatography column (Merck) for protein capture. The resin was sufficiently washed with PBS and the protein was eluted with wash buffer supplemented with reduced glutathione. The eluted proteins were concentrated and further purified by size exclusion chromatography (Superdex 200 Increase 10/300GL) with a buffer containing 20 mM Tris pH 8.0, 250 mM NaCl. The fractions containing target proteins were pooled and concentrated for mass spectrometry analysis.

Mass spectrometry validation of purified NPC1-I protein

The purified NPC1-I protein was validated by Orbitrap Fusion MS (Thermo Fisher, San Jose, CA) using Proteome Discoverer 2.2 and Xcalibur analysis software at the Analytical Chemistry Platform at SIAIS, ShanghaiTech University. The entire gels were rinsed with water for 3–4 h, then the bands of GST (control, $n = 1$) and NPC-I (sample, $n = 1$) were excised with a clean scalpel. The two excised bands were cut into cubes (1 mm × 1 mm) separately. The gel slices were transferred into two microcentrifuge tubes and spun down by a microcentrifuge. For in-gel reduction, alkylation, and de-staining, the gels were incubated with 100 µL de-staining solution (100 mM ammonium bicarbonate buffer containing 50% acetonitrile, vol/vol) for 30 min at 37 °C, and then incubated with 500 µL neat acetonitrile for 10 min until gel slices shrank and became opaque and stiff. These gel slices were span to remove all liquid and 40 µL of 10 mM DTT solution was added to cover gel slices for 30 min at 56 °C in an air thermostat. The tubes were chilled down to room temperature, and incubated with 500 µL acetonitrile for 10 min and then all liquid was removed. The gels were incubated with 40 µL of 55 mM iodoacetamide solution for 20 min at room temperature in the dark, treated with acetonitrile, and then all liquid removed. The dry gels were incubated with 70 µL trypsin buffer containing 13 µg/mL trypsin for 100 min at 4 °C and then incubated with 20 µL 100 mM ammonium bicarbonate containing 10% (vol/vol) acetonitrile at 37 °C overnight. The next day the samples were incubated with 200 µL extraction buffer (1 vol: 2 vol of 5% formic acid: acetonitrile) for 15 min at 37 °C in a shaker. Then the supernatant was collected into a PCR tube, dried in a vacuum centrifuge, and stored at 4 °C for further analysis.

For liquid chromatography (LC) analysis, the above samples were supplemented with 20 µL of 0.1% (vol/vol) formic acid, vortexed, and

centrifuged for 5 min at 12,000 × *g*. These treated peptides were loaded onto an analytical column (Ionopticks, AUR2-25075C18A, 25 cm × 75 µm, C18, 1.6 µm) connected to an Easy-nLC1200 UHPLC-Orbitrap Fusion (Thermo Fisher Scientific). The elution gradient and mobile phase constitution used for peptide separation were set as follows: 0–60 min, 5–30% buffer B; 60–70 min, 30–45% buffer B; 70–75 min, 45–100% buffer B; 75–80 min, 100% buffer B at a flow rate of 300 nL/min. Mobile phase in buffer A was 0.1% formic acid in water and mobile phase in buffer B was 0.1% formic acid in 80% acetonitrile.

Peptides eluted from the LC column were directly electro-sprayed into the mass spectrometer with the application of a distal 2.1 kV spray voltage. Survey full-scan mass spectra (from m/z 350 to 1800) were acquired in the Orbitrap analyzer (Orbitrap Fusion, Thermo Fisher Scientific) with resolution $r = 60{,}000$ at m/z 400. The cycle time of the MS-MS2 events was 3 s, sequentially generated and selected from the full mass spectrum at a 32% normalized collision energy. The dynamic exclusion time was set to 10 s. The acquired MS/MS data were analyzed using the AA sequence of protein GST, using Protein Discoverer 2.2 with the parameter settings as follows: precursor and fragment mass tolerance of 10 ppm and 0.02 Da and dynamic modifications of + 15.995 Da for Oxidation (Met) and + 42.011 Da for Acetyl (N-terminus), and + 57.021 Da for Carbamidomethyl (C terminus) as static modifications. To accurately estimate peptide probabilities and filter the false discovery, the fixed value PSM validator node was used and set to have a maximum delta Cn of 0.05. Trypsin was defined as cleavage enzyme and the maximal number of missed cleavage sites was set to two.

Far western blotting

Far western blotting was performed as previously described[97]. Briefly, 0.2–1 µg purified NPC1-I protein (with an unknown impurity band) or a control GST protein was mixed with SDS-PAGE loading buffer (Takara) containing 200 mM DTT, incubated at 95 °C for 10 min and resolved on 4–12% PAGE gels (GenScript, Nanjing, China). Protein samples were transferred onto nitrocellulose (PVDF) membranes (Merck) using an iBlot gel transfer system (Thermo). PVDF membrane was treated with PBS solution containing gradient concentrations of guanidine hydrochloride (GuHCl) solution (Solarbio, China) for protein unfolding and refolding. The GuHCl gradient was decreased from 6 M to 3 M and then 0.1 M with the membrane being treated with each gradient for 30 min. Finally, the membrane was treated with PBS without GuHCl at 4 °C overnight. The membrane was then blocked with PBS containing 5% milk (w/v) and incubated with 1–10 µg GP64 protein (SinoBiological, Beijing, China) overnight at 4 °C. The membrane was then treated with an anti-GP64 mouse antibody (Abcam, Cat. No. ab91214) as the primary antibody and an HRP-conjugated anti-mouse antibody (R&D, Cat. No. HAF007) as the secondary antibody. The bait protein could be detected at the location of the prey protein on the membrane if they interact to form a complex.

Transduction with DiOC18-labeled baculovirus

Baculovirus was labeled with DiOC18 (Thermo) at a final concentration of 2 µM in PBS. The solution was rotated at room temperature in the dark for 1 h and then filtered through a 0.22 µm pore size syringe filter (Merck) to remove unbound dyes and aggregates. Cells were infected with DiOC18-labeled baculovirus at 37 °C for 3 h, then washed with PBS three times and treated with trypsin briefly to remove free and surface-bound viruses. Thereafter, the cells were fixed with PFA and analyzed by flow cytometry (CytoFLEX, Beckman Coulter, California, USA) and confocal microscopy (LSM 710, Zeiss, Oberkochen, Germany). A control group with DiOC18 dye alone, without the addition of baculovirus, was prepared following the same filtration process as described above to assess the background fluorescence labeling of cells by free dyes in the DiOC18-Bac-EGFP-treated groups.

Baculovirus transduction in mice

Npc1$^{-/+}$ and wild-type C57BL/6 mice were purchased from, bred, and raised in GemPharmatech (Nanjing, China). All mice were housed in animal facility with ambient room temperature of 20–26 °C, humidity of 50–70%, and dark/light cycle of 12 h. Baculovirus-related animal experiments were performed in OBiO-tech corporation (Shanghai, China). For baculovirus, transduction, 6–8-week-old male *Npc1*$^{-/+}$ and wild-type C57BL/6 mice were used. The mice were maintained within a Specific Pathogen-Free (SPF) facility with free access to water and food. The housing facility for mice was under a 12:12 h light: dark cycle at temperatures 20–26 °C, humidity 40–70%. For transduction experiments, mice were randomly grouped ($n = 3$ to 9 per group as indicated) and injected with baculoviruses through tail vein with a dose of 4.4×10^4 IU per gram body weight. Animals were sacrificed under an anesthetic condition at the indicated time post-baculovirus transduction. The tissues including liver, brain, spleen, lung, and kidney were collected and flash-frozen in liquid nitrogen or fixed in PFA buffer for further analyses.

For tissue tropism of Bac-EGFP transduction, Bac-EGFP-transduced tissues were flash-frozen and fixed with optimal cutting temperature compound (OCT). The fixed tissues were sectioned at 5 µm, and the sections were fixed with PFA and stained with Hoechst (Thermo). The fluorescence images were acquired using confocal microscopy (LSM 710, Zeiss).

Statistics and reproducibility

All data were the results from at least three biological replicates and were shown as mean ± standard deviation unless noted otherwise. All experiments were repeated three times independently (biological replicates) unless noted otherwise. No data were excluded for analyses. Statistical analyses and graphing were performed with GraphPad Prism 7.0. The *P*-values were determined using two-tailed unpaired Student's t-test unless otherwise noted.

Reporting summary

Further information on research design is available in the Nature Portfolio Reporting Summary linked to this article.

Data availability

The authors declare that all data supporting the findings of this study are available in the article, its Supplementary Data, its Source Data, or from the corresponding authors upon request. Source data are provided with this paper. The NGS data generated in this study have been deposited in the SRA database under accession code PRJNA1131913. Source data are provided with this paper.

References

1. Ihalainen, T. O. et al. Morphological characterization of baculovirus Autographa californica multiple nucleopolyhedrovirus. *Virus Res.* **148**, 71–74 (2010).
2. Ayres, M. D., Howard, S. C., Kuzio, J., Lopez-Ferber, M. & Possee, R. D. The complete DNA sequence of Autographa californica nuclear polyhedrosis virus. *Virology* **202**, 586–605 (1994).
3. Rohrmann, G. F. Baculovirus structural proteins. *J. Gen. Virol.* **73**, 749–761 (1992).
4. Summers, M. D. & Volkman, L. E. Comparison of biophysical and morphological properties of occluded and extracellular non-occluded baculovirus from in vivo and in vitro host systems. *J. Virol.* **17**, 962–972 (1976).
5. Blissard, G. W. & Rohrmann, G. F. Location, sequence, transcriptional mapping, and temporal expression of the gp64 envelope glycoprotein gene of the Orgyia pseudotsugata multicapsid nuclear polyhedrosis virus. *Virology* **170**, 537–555 (1989).

6. Peng, K. et al. Characterization of novel components of the baculovirus per os infectivity factor complex. *J. Virol.* **86**, 4981–4988 (2012).
7. Peng, K., van Oers, M. M., Hu, Z., van Lent, J. W. & Vlak, J. M. Baculovirus per os infectivity factors form a complex on the surface of occlusion-derived virus. *J. Virol.* **84**, 9497–9504 (2010).
8. Volkman, L. E. & Summers, M. D. Autographa californica nuclear polyhedrosis virus: comparative infectivity of the occluded, alkali-liberated, and nonoccluded forms. *J. Invertebr. Pathol.* **30**, 102–103 (1977).
9. Summers, M. D. Electron microscopic observations on granulosis virus entry, uncoating and replication processes during infection of the midgut cells of Trichoplusia ni. *J. Ultrastruct.* **35**, 606–625 (1971).
10. Zhou, J. & Blissard, G. W. Identification of a GP64 subdomain involved in receptor binding by budded virions of the baculovirus Autographica californica multicapsid nucleopolyhedrovirus. *J. Virol.* **82**, 4449–4460 (2008).
11. Long, G., Pan, X., Kormelink, R. & Vlak, J. M. Functional entry of baculovirus into insect and mammalian cells is dependent on clathrin-mediated endocytosis. *J. Virol.* **80**, 8830–8833 (2006).
12. Granados, R. R. & Lawler, K. A. In vivo pathway of Autographa californica baculovirus invasion and infection. *Virology* **108**, 297–308 (1981).
13. Horton, H. M. & Burand, J. P. Saturable attachment sites for polyhedron-derived baculovirus on insect cells and evidence for entry via direct membrane fusion. *J. Virol.* **67**, 1860–1868 (1993).
14. Pearson, M. N., Russell, R. L. & Rohrmann, G. F. Characterization of a baculovirus-encoded protein that is associated with infected-cell membranes and budded virions. *Virology* **291**, 22–31 (2001).
15. Lung, O. Y., Cruz-Alvarez, M. & Blissard, G. W. Ac23, an envelope fusion protein homolog in the baculovirus Autographa californica multicapsid nucleopolyhedrovirus, is a viral pathogenicity factor. *J. Virol.* **77**, 328–339 (2003).
16. WF, I. J. et al. A novel baculovirus envelope fusion protein with a proprotein convertase cleavage site. *Virology* **275**, 30–41 (2000).
17. Long, G., Pan, X., Westenberg, M. & Vlak, J. M. Functional role of the cytoplasmic tail domain of the major envelope fusion protein of group II baculoviruses. *J. Virol.* **80**, 11226–11234 (2006).
18. Westenberg, M. et al. Functional analysis of the putative fusion domain of the baculovirus envelope fusion protein F. *J. Virol.* **78**, 6946–6954 (2004).
19. Kadlec, J., Loureiro, S., Abrescia, N. G., Stuart, D. I. & Jones, I. M. The postfusion structure of baculovirus gp64 supports a unified view of viral fusion machines. *Nat. Struct. Mol. Biol.* **15**, 1024–1030 (2008).
20. White, J. M., Delos, S. E., Brecher, M. & Schornberg, K. Structures and mechanisms of viral membrane fusion proteins: multiple variations on a common theme. *Crit. Rev. Biochem.* **43**, 189–219 (2008).
21. Blissard, G. W. & Wenz, J. R. Baculovirus gp64 envelope glycoprotein is sufficient to mediate pH-dependent membrane fusion. *J. Virol.* **66**, 6829–6835 (1992).
22. Zhou, J. & Blissard, G. W. Mapping the conformational epitope of a neutralizing antibody (AcV1) directed against the AcMNPV GP64 protein. *Virology* **352**, 427–437 (2006).
23. Rohrmann, G. F. The AcMNPV genome: gene content, conservation, and function. in *Baculovirus Molecular Biology*, 3rd edn, 1–48 (National Center for Biotechnology Information. Bethesda, MD, 2013).
24. Smith, G. E., Summers, M. D. & Fraser, M. J. Production of human beta interferon in insect cells infected with a baculovirus expression vector. *MCB* **3**, 2156–2165 (1983).
25. Potter, K. N., Li, Y. & Capra, J. D. Antibody production in the baculovirus expression system. *Int Rev. Immunol.* **10**, 103–112 (1993).
26. Gheysen, D. et al. Assembly and release of HIV-1 precursor Pr55gag virus-like particles from recombinant baculovirus-infected insect cells. *Cell* **59**, 103–112 (1989).
27. Malogolovkin, A. et al. Enhanced Zika virus-like particle development using Baculovirus spp. constructs. *J. Med. Virol.* **95**, e28252 (2023).
28. Kim, C. H. et al. Direct vaccination with pseudotype baculovirus expressing murine telomerase induces anti-tumor immunity comparable with RNA-electroporated dendritic cells in a murine glioma model. *Cancer Lett.* **250**, 276–283 (2007).
29. Fan, H. et al. Construction and immunogenicity of recombinant pseudotype baculovirus expressing the capsid protein of porcine circovirus type 2 in mice. *J. Virol. Methods* **150**, 21–26 (2008).
30. Huang, H. et al. Construction and immunogenicity of a recombinant pseudotype baculovirus expressing the glycoprotein of rabies virus in mice. *Arch. Virol.* **156**, 753–758 (2011).
31. Wang, S. et al. Construction and immunogenicity of pseudotype baculovirus expressing GP5 and M protein of porcine reproductive and respiratory syndrome virus. *Vaccine* **25**, 8220–8227 (2007).
32. Fang, R. et al. Construction and immunogenicity of pseudotype baculovirus expressing Toxoplasma gondii SAG1 protein in BALB/c mice model. *Vaccine* **28**, 1803–1807 (2010).
33. Grabowska, A. K. et al. New baculovirus recombinants expressing Pseudorabies virus (PRV) glycoproteins protect mice against lethal challenge infection. *Vaccine* **27**, 3584–3591 (2009).
34. Chen, C. Y., Lin, C. Y., Chen, G. Y. & Hu, Y. C. Baculovirus as a gene delivery vector: recent understandings of molecular alterations in transduced cells and latest applications. *Biotechnol. Adv.* **29**, 618–631 (2011).
35. Makkonen, K. E., Airenne, K. & Ylä-Herttulala, S. Baculovirus-mediated gene delivery and RNAi applications. *Viruses* **7**, 2099–2125 (2015).
36. Mansouri, M. & Berger, P. Baculovirus for gene delivery to mammalian cells: Past, present and future. *Plasmid* **98**, 1–7 (2018).
37. Lei, Y. et al. Gene editing of human embryonic stem cells via an engineered baculoviral vector carrying zinc-finger nucleases. *Mol. Ther.* **19**, 942–950 (2011).
38. Tay, F. C. et al. Targeted transgene insertion into the AAVS1 locus driven by baculoviral vector-mediated zinc finger nuclease expression in human-induced pluripotent stem cells. *J. Gene Med.* **15**, 384–395 (2013).
39. Phang, R. Z. et al. Zinc finger nuclease-expressing baculoviral vectors mediate targeted genome integration of reprogramming factor genes to facilitate the generation of human induced pluripotent stem cells. *Stem Cells Transl. Med.* **2**, 935–945 (2013).
40. Zhu, H. et al. Baculoviral transduction facilitates TALEN-mediated targeted transgene integration and Cre/LoxP cassette exchange in human-induced pluripotent stem cells. *Nucleic Acids Res.* **41**, e180 (2013).
41. Hindriksen, S. et al. Baculoviral delivery of CRISPR/Cas9 facilitates efficient genome editing in human cells. *PLoS One* **12**, e0179514 (2017).
42. Aulicino, F. et al. Highly efficient CRISPR-mediated large DNA docking and multiplexed prime editing using a single baculovirus. *Nucleic Acids Res.* **50**, 7783–7799 (2022).
43. Nguyen, G. N. et al. A long-term study of AAV gene therapy in dogs with hemophilia A identifies clonal expansions of transduced liver cells. *Nat. Biotechnol.* **39**, 47–55 (2021).
44. McCarty, D. M., Young, S. M. Jr. & Samulski, R. J. Integration of adeno-associated virus (AAV) and recombinant AAV vectors. *Annu Rev. Genet.* **38**, 819–845 (2004).
45. Sarkis, C. et al. Efficient transduction of neural cells in vitro and in vivo by a baculovirus-derived vector. *Proc. Natl Acad. Sci. USA* **97**, 14638–14643 (2000).
46. Turunen, T. A., Laakkonen, J. P., Alasaarela, L., Airenne, K. J. & Ylä-Herttuala, S. Sleeping Beauty-baculovirus hybrid vectors for long-term gene expression in the eye. *J. Gene Med.* **16**, 40–53 (2014).

47. Kinnunen, K. et al. Baculovirus is an efficient vector for the transduction of the eye: comparison of baculovirus- and adenovirus-mediated intravitreal vascular endothelial growth factor D gene transfer in the rabbit eye. *J. Gene Med.* **11**, 382–389 (2009).
48. Luo, W. Y. et al. Baculovirus vectors for antiangiogenesis-based cancer gene therapy. *Cancer Gene Ther.* **18**, 637–645 (2011).
49. Luo, W. Y. et al. Development of the hybrid Sleeping Beauty: baculovirus vector for sustained gene expression and cancer therapy. *Gene Ther.* **19**, 844–851 (2012).
50. Liu, Z. et al. Surface displaying of swine IgG1 Fc enhances baculovirus-vectored vaccine efficacy by facilitating viral complement escape and mammalian cell transduction. *Vet. Res.* **48**, 29 (2017).
51. Hu, L. et al. Improving baculovirus transduction of mammalian cells by incorporation of thogotovirus glycoproteins. *Virol. Sin.* **34**, 454–466 (2019).
52. Pieroni, L., Maione, D. & La Monica, N. In vivo gene transfer in mouse skeletal muscle mediated by baculovirus vectors. *Hum. Gene Ther.* **12**, 871–881 (2001).
53. Barsoum, J., Brown, R., McKee, M. & Boyce, F. M. Efficient transduction of mammalian cells by a recombinant baculovirus having the vesicular stomatitis virus G glycoprotein. *Hum. Gene Ther.* **8**, 2011–2018 (1997).
54. Duisit, G. et al. Baculovirus vector requires electrostatic interactions including heparan sulfate for efficient gene transfer in mammalian cells. *J. Gene Med.* **1**, 93–102 (1999).
55. Wu, C. & Wang, S. A pH-sensitive heparin-binding sequence from Baculovirus gp64 protein is important for binding to mammalian cells but not to Sf9 insect cells. *J. Virol.* **86**, 484–491 (2012).
56. Makkonen, K. E. et al. 6-o- and N-sulfated syndecan-1 promotes baculovirus binding and entry into Mammalian cells. *J. Virol.* **87**, 11148–11159 (2013).
57. Tani, H., Nishijima, M., Ushijima, H., Miyamura, T. & Matsuura, Y. Characterization of cell-surface determinants important for baculovirus infection. *Virology* **279**, 343–353 (2001).
58. Luz-Madrigal, A., Asanov, A., Camacho-Zarco, A. R., Sampieri, A. & Vaca, L. A cholesterol recognition amino acid consensus domain in GP64 fusion protein facilitates anchoring of baculovirus to mammalian cells. *J. Virol.* **87**, 11894–11907 (2013).
59. Kataoka, C. et al. Baculovirus GP64-mediated entry into mammalian cells. *J. Virol.* **86**, 2610–2620 (2012).
60. Amalfi, S. et al. Baculovirus transduction in mammalian cells is affected by the production of type I and III interferons, which is mediated mainly by the cGAS-STING pathway. *J. Virol.* **94**, e01555-20 (2020).
61. Puschnik, A. S., Majzoub, K., Ooi, Y. S. & Carette, J. E. A CRISPR toolbox to study virus-host interactions. *Nat. Rev. Microbiol.* **15**, 351–364 (2017).
62. Mei, H. et al. Surfaceome CRISPR screen identifies OLFML3 as a rhinovirus-inducible IFN antagonist. *Genome Biol.* **22**, 297 (2021).
63. Shalem, O. et al. Genome-scale CRISPR-Cas9 knockout screening in human cells. *Science* **343**, 84–87 (2014).
64. Clausen, T. M. et al. SARS-CoV-2 infection depends on cellular heparan sulfate and ACE2. *Cell* **183**, 1043–1057.e1015 (2020).
65. Shukla, D. et al. A novel role for 3-O-sulfated heparan sulfate in herpes simplex virus 1 entry. *Cell* **99**, 13–22 (1999).
66. Chen, Y. et al. Dengue virus infectivity depends on envelope protein binding to target cell heparan sulfate. *Nat. Med.* **3**, 866–871 (1997).
67. Carette, J. E. et al. Ebola virus entry requires the cholesterol transporter Niemann-Pick C1. *Nature* **477**, 340–343 (2011).
68. King, L. B. et al. The Marburgvirus-neutralizing human monoclonal antibody MR191 targets a conserved site to block virus receptor binding. *Cell Host Microbe* **23**, 101–109.e104 (2018).
69. Tjia, S. T., zu Altenschildesche, G. M. & Doerfler, W. Autographa californica nuclear polyhedrosis virus (AcNPV) DNA does not persist in mass cultures of mammalian cells. *Virology* **125**, 107–117 (1983).
70. Bowman, E. J., Siebers, A. & Altendorf, K. Bafilomycins: a class of inhibitors of membrane ATPases from microorganisms, animal cells, and plant cells. *Proc. Natl Acad. Sci. USA* **85**, 7972–7976 (1988).
71. Zhao, H. et al. A broad-spectrum virus- and host-targeting peptide against respiratory viruses including influenza virus and SARS-CoV-2. *Nat. Commun.* **11**, 4252 (2020).
72. Shang, C. et al. Inhibitors of endosomal acidification suppress SARS-CoV-2 replication and relieve viral pneumonia in hACE2 transgenic mice. *Virol. J.* **18**, 46 (2021).
73. Yamada, S. Specific functions of Exostosin-like 3 (EXTL3) gene products. *Cell Mol. Biol. Lett.* **25**, 39 (2020).
74. Awad, W., Kjellström, S., Svensson Birkedal, G., Mani, K. & Logan, D. T. Structural and biophysical characterization of human EXTL3: domain organization, glycosylation, and solution structure. *Biochemistry* **57**, 1166–1177 (2018).
75. Dogra, P. et al. Novel heparan sulfate-binding peptides for blocking herpesvirus entry. *PLoS One* **10**, e0126239 (2015).
76. Sarrazin, S., Lamanna, W. C. & Esko, J. D. Heparan sulfate proteoglycans. *Cold Spring Harb. Perspect. Biol.* **3**, a004952 (2011).
77. Giraldo, M. I. et al. Envelope protein ubiquitination drives entry and pathogenesis of Zika virus. *Nature* **585**, 414–419 (2020).
78. Banerjee, I. et al. Influenza A virus uses the aggresome processing machinery for host cell entry. *Science* **346**, 473–477 (2014).
79. Davies, J. P., Chen, F. W. & Ioannou, Y. A. Transmembrane molecular pump activity of Niemann-Pick C1 protein. *Science* **290**, 2295–2298 (2000).
80. Wang, H. et al. Ebola viral glycoprotein bound to its endosomal receptor Niemann-Pick C1. *Cell* **164**, 258–268 (2016).
81. Gong, X. et al. Structural insights into the Niemann-Pick C1 (NPC1)-mediated cholesterol transfer and Ebola infection. *Cell* **165**, 1467–1478 (2016).
82. Santiago-Mujica, E. et al. Hepatic and neuronal phenotype of NPC1(−/−) mice. *Heliyon* **5**, e01293 (2019).
83. Berger, I., Fitzgerald, D. J. & Richmond, T. J. Baculovirus expression system for heterologous multiprotein complexes. *Nat. Biotechnol.* **22**, 1583–1587 (2004).
84. Fitzgerald, D. J. et al. Protein complex expression by using multigene baculoviral vectors. *Nat. Methods* **3**, 1021–1032 (2006).
85. Bieniossek, C. et al. Automated unrestricted multigene recombineering for multiprotein complex production. *Nat. Methods* **6**, 447–450 (2009).
86. Hunt, C. L., Lennemann, N. J. & Maury, W. Filovirus entry: a novelty in the viral fusion world. *Viruses* **4**, 258–275 (2012).
87. Cuesta-Geijo, M. et al. New insights into the role of endosomal proteins for African swine fever virus infection. *Plos Pathog.* **18**, e1009784 (2022).
88. Fan, Y. et al. The NPC families mediate BmNPV entry. *Microbiol. Spectr.* **10**, e0091722 (2022).
89. Li, Z. et al. Baculovirus utilizes cholesterol transporter Niemann-Pick C1 for host cell entry. *Front. Microbiol.* **10**, 2825 (2019).
90. Ye, J., Davé, U. P., Grishin, N. V., Goldstein, J. L. & Brown, M. S. Asparagine-proline sequence within membrane-spanning segment of SREBP triggers intramembrane cleavage by site-2 protease. *Proc. Natl Acad. Sci. USA* **97**, 5123–5128 (2000).
91. Ye, J. et al. ER stress induces cleavage of membrane-bound ATF6 by the same proteases that process SREBPs. *Mol. Cell* **6**, 1355–1364 (2000).
92. Denard, B. et al. The membrane-bound transcription factor CREB3L1 is activated in response to virus infection to inhibit proliferation of virus-infected cells. *Cell Host Microbe* **10**, 65–74 (2011).

93. Amalfi, S. et al. P26 enhances baculovirus gene delivery by modulating the mammalian antiviral response. *Appl. Microbiol Biot*. **107**, 6277–6286 (2023).
94. Reed, L. J. & Muench, H. A Simple method of estimating fifty percent endpoints. *Am. J. Epidemiol.* **27**, 493–497 (1938).
95. Brinkman, E. K. et al. Easy quantification of template-directed CRISPR/Cas9 editing. *Nucleic Acids Res.* **46**, e58 (2018).
96. Xu, Z. S. et al. LDLR is an entry receptor for Crimean-Congo hemorrhagic fever virus. *Cell Res.* **34**, 140–150 (2024).
97. Wu, Y., Li, Q. & Chen, X. Z. Detecting protein-protein interactions by Far western blotting. *Nat. Protoc.* **2**, 3278–3284 (2007).

Acknowledgements

We thank Lishuang Zhang and Pengwei Zhang from the Discovery Technology Platform of SIAIS for the support of flow cytometry experiments, Wei Zhu from the Analytical Chemistry Platform for assistance with mass spectrometry analysis, and the Biomedical Big Data Platform for the design of sgRNA libraries and MAGeCK analyses. This research was supported by the Science and Technology Commission of Shanghai Municipality (23ZR1442100 to J.L.), the Shanghai Frontiers Science Center for Biomacromolecules and Precision Medicine at ShanghaiTech University (2022A0301-417-01 to J.L.), and the Postgraduate Scientific Research Innovation Project of Central South University (2023ZZTS0542 to Y.H.).

Author contributions

J.L., J.D.L., and H.M. conceived this study, J.L., H.M., Y.H., and Y.N. designed the experiments, and Y.H., H.M., C.D., and C.Y. carried out the experiments and analyzed the data. W.W., H.M., and L.J. designed the sgRNA libraries, and Y.H., H.M., J.L, and J.D.L. wrote the manuscript. All authors contributed to the manuscript and approved the submission.

Competing interests

J. Liu is the founder and shareholder of Shanghai AsiFlyer Biotechnology. The remaining authors declare no competing interests.

Ethical approval

All study protocols involving mice were approved by the ethical committee of ShanghaiTech University (approval number: 20230821001) and conducted in accordance with regulatory policies in China for the care and use of animals.

Additional information

Supplementary information The online version contains supplementary material available at https://doi.org/10.1038/s41467-024-52193-w.

Correspondence and requests for materials should be addressed to Hong Mei, Jia-Da Li or Jia Liu.

Peer review information *Nature Communications* thanks Francesco Aulicino and the other, anonymous, reviewer(s) for their contribution to the peer review of this work. A peer review file is available.